The Photometric Analysis of SN 2025mvn

Abstract

We observed the target SN 2025mvn, a supernova discovered on June 6th, 2025, located within the spiral galaxy NGC 5033. This supernova was imaged, stacked, and extracted for data such as magnitudes, calibration stars, and Sloan gs and rs. This data was used to model a light curve to explain the lifespan of the supernova. Based on the observations and calculations from such processes, it can be concluded that SN 2025mvn is a likely Type IIb supernova that is significantly brighter in the red part of the visible light spectrum than the green. The light curve created off of the data collected over these past four weeks provided the evidence for these conclusions.

Introduction

The past month has consisted of observational research on the extragalactic supernova 2025mvn in the galaxy NGC 5033. This was accomplished through the use of the 0.4m telescope at the Leitner Family Observatory and Planetarium and the T24 telescope at the Sierra Remote Observatory through iTelescope. SN 2025mvn was captured south of the galactic nucleus with its host galaxy NGC 5033, which has a magnitude of 10.75 (Rochester (2025)) (**Figure 1**). NGC 5033 is a spiral galaxy 40 million light-years away and is approximately 30,660 parsecs wide(ESA (2018)). SN 2025mvn was discovered on June 6th, 2025, and since early July has been carefully studied to extract relevant data to aid in astronomers' understanding of stellar and galactic evolution. Software such as AstroImageJ, Siril, and SaoImage DS9 were used to visualize the target, and Python scripts were written to extract data on the supernova and surrounding calibration stars.

Figure 1: A monochrome Charge-Coupled Device (CDD) image of SN 2025mvn taken on the T24 Sierra Remote Observatory at Auberry California USA - MPC U69 through iTelescope Network on July 13th, 2025 (Support, 2021). The supernova is marked with a white vertical and horizontal line near the host galaxy NGC 5033.

The purpose of studying supernovae, specifically in other galaxies, is to better understand the life cycle of stars and processes involving heavy elements. It also gives insights on galactic evolution, and the chemical composition and structure of distant galaxies. By making a light curve of the data gathered over the past four weeks, the type of supernova can be determined, which further expands on previous understanding of extragalactic objects. Such models are crucial for calculating the brightness over a certain period of time, which allows the distance and luminosity of an object to be calculated (B. Mattson et al. (2013)). This research paper will cover the methods that were used to gather data on the supernova 2025mvn, such as its color magnitudes, light curve, and categorization.

Methods

Images of SN 2025mvn were collected in the past four weeks to construct a light curve and provide crucial information about the supernova, such as its classification and changing color magnitudes. SN 2025mvn has a Right Ascension (RA) of 13hrs 13mins 27.881s and a Declination (Dec) of +36° 35' 11.71''. Data were gathered from two sources: the 0.4 meter Ritchey-Chretien Telescope located at Leitner Family Observatory and Planetarium, along with the T24 Sierra Remote Observatory telescope through iTelescope. Few technical issues occurred, but there were two major ones: the slewing being incorrect on the 0.4m telescope and the iTelescope telescopes not returning data. There was no fix for the lack of data, but the slewing was fixed whenever possible to resume data collection. Though these issues did push back progress, a total of ten nights of data were successfully collected (**Table 1**).

At LFOP, the process of collecting data started with calibration, which was achieved by slewing to Arcturus, focusing, and then slewing to the J2000 RA and Dec of SN 2025mvn. Images were taken through the Sloan g and Sloan r filters, with the majority of the collected frames having an exposure time of 30 through 60 seconds. The images collected from the telescopes were registered, calibrated, and stacked using Siril to make them analyzable. APASS provided the calibration stars for each iteration of images. The images, already stacked to FITS files, were then outfitted with the World Coordinate System (WCS) to imprint the right ascension and declination onto each file.

Using the ten observational data points, a multi-step photometric analysis was performed to find the standard magnitude of SN 2025mvn in both red and green filters. First, the green and red fluxes for the calibration stars were calculated in each image. The coordinates of the calibration stars were gathered by using the APASS DR10 Download from AVASSO. Each day of data containing a Sloan g and Sloan r fit images required their own CSV file due to altering centers and field of views (FOVs) in each image and used to locate the calibration stars on the fit files. Each APASS file was cropped during this process, as some stars included in the CSV file were out of range in the images collected. With the final edited CSV file, the RAs and Decs were used to locate the calibration stars on the fit images. After the fluxes were calculated for both the green and red images, the instrumental magnitudes for each calibration star were calculated through the use of the equation:

$$m = -2.5log(b)$$

Where m is the magnitude of the star, while b is the observed brightness of the star. Offset would've been added in the general form of the equation, but was assumed to be 0 to solve for instrumental magnitude.

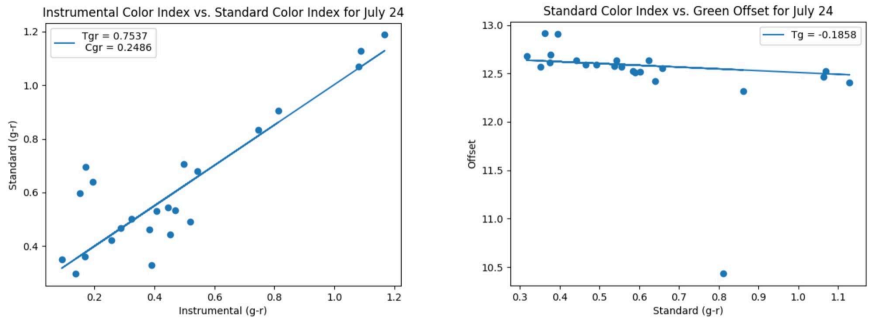

Figure 2: Standard vs. Instrumental and Standard (g-r) vs. green offset of APASS calibration stars with calculated apparent magnitudes. These are images taken on July 24. The linear line represents the least-squares regression(LSR) line of uncalibrated magnitudes obtained through photometric analysis of SN 2025mvn. The left graph compares the standard and instrumental color indices of the calibration stars, determining the atmospheric effects. The graph on the right shows green offset varying with standard color index (g-r), determining the color term correction (Aavso.org. (2020)).

After solving for the instrumental magnitudes of each star, the color index calculation was performed, given by Inst g-Inst r. The color index was then used in a system of two transformation equations:

$$Std(g - r) = Tgr * Inst(g - r) + Cgr$$

$$Std(g) - Inst(g) = Tg * Std(g - r) + Cg$$

Where for Equation 1, *Std(g-r)* is the standard color index; *Inst(g-r)* is the instrumental color; *Tgr* is the transformation coefficient; and *Cgr* is the color offset. For Equation 2, *Std(g)* is the standard magnitude in g; *Inst(g)* is the instrumental magnitude in g; *Tg* is the green-band transformation slope; and *Cg* is the green-band offset.

Performing least-squares regression, the slope and intercept for both equations were calculated, with the two regressions having standard errors, Eq1 and Eq2 respectively, associated with them. The slopes and intercepts were then used as *Tg*, *Tgr*, *Cg*, and *Cgr* in the same equations to analyze the atmospheric effects and color correction of the calculated apparent magnitudes (**Figure 2**) and solve for the standard magnitudes of SN 2025mvn. With the calculated *Std(g-r)* and *Std(g)* from the transformation equations, the simple equation was used to find *Std(r)*:

$$Std(g) - Std(g - r) = Std(r)$$

was used to solve for the standard red magnitude of SN 2025mvn.

The uncertainty that resulted from finding the standard g magnitude of SN 2025mvn was $(\sigma_1^2+\sigma_2^2)^{0.5}$, where σ_1 is the error calculated from Equation 1, and σ_2 is the error calculated from Equation 2. Since both equations were used to find the magnitude, the error compounds are in quadrature. Following similar logic, since the standard r magnitude was calculated via the difference of standard

green magnitude and green minus red magnitude, its error is $(2\sigma_1^2+\sigma^2_2)^{0.5}$ which is greater than the standard green magnitude because it wasn't computed directly from the data. Therefore, the supernova light curve fitting representing the light curve of SN 2025mvn over the observation period was modeled with the standard g magnitude.

The final ten calculated apparent magnitudes of SN 2025mvn would be graphed and compared to five light curve model fits using Chi-Squared to determine which type of supernova SN 2025mvn would best fit. Once the best-fit light curve was found, a generalized fit of a chi-squared analysis for 40,000 different values of distance moduli and plotting a contour color map was performed to identify the best estimate for the day of peak brightness and the distance modulus of SN 2025mvn. With the x-shift of the contour map, the following equation could be used to find the total distance in parsecs Sn 2025mvn is from earth:

$$m - M = 5log(d) - 5$$

Where *m-M* is the apparent magnitude minus the absolute magnitude, also known as the distance moduli, and *d* is the total distance the object is away from Earth in parsecs. From this, the distance modulus, distance in parsecs, and the peak date of SN 2025mvn could be found. Together, these quantitative and qualitative procedures were used to provide a comprehensive understanding of SN 2025mvn.

Results

To determine the type, the apparent magnitudes of SN 2025mvn at each of the 10 observations conducted during the 4-week period (**Table 2**) was fitted into different light curve models of Type I and Type II supernova types (**Figure 4**). The upwards, downwards, and then upwards trend resembles the light curve of Type IIb supernovae with the lowest chi-squared value of 1.501, whereas the other light curve chi-squared values averaged around 6.575 (**Table 4**). Due to significant atmospheric effects and weak filter sets, there were weak calculations evident by analyzing the calculated slopes and intercepts (**Table 3**). Therefore, a second test was run omitting high-error points and recalculating the light curve fits with the same process used before. The results conclude that Type IIb continues to be the best fit with a Chi-Squared of 1.080, where other light curve fits averaged a chi-squared of 3.977. Therefore, even with weak observations omitted (specifically, July 15th, 20th, 25th, and the 27th were omitted due to weak Tgr, Cgr, and Tg results), the best light curve fit continues to fit Type IIb, solidifying that the most accurate calculated apparent magnitudes of SN 2025mvn resembles Type IIb supernova.

By using a generalized fit of chi-squared analysis, the identified best-fit estimate for the distance modulus of SN 2025mvn and the peak date could be determined. The darkest area of the graph represents the lowest level of uncertainty and therefore the best distance modulus and y-shift of the data. The darkest and best-fit estimate for the x-shift was approximately -34.673 ± 0.075, with a y-shift of approximately 2460873.267 ± 0.26 (**Figure 3**). Thus, we can conclude the peak of SN 2025mvn occurred on 2460873.267 ± 0.26 Julian Day Number. Using the difference of the apparent and standard magnitude (the x-shift of the graph), the distance of the supernova could be calculated to be $1.165 \pm 0.039 \times 10^{-6}$ parsecs away from Earth.

Although poor weather, light pollution, and telescope misuse may have worsened clarity, the model indicates that SN 2025mvn peaked on the Julian Date 2460873.267 (July 16th, 2025) with corresponding magnitudes of roughly 17.423 Sloan green magnitude and 16.854 Sloan red magnitude. Therefore, the trend of the calculated magnitudes supports that SN 2025mvn best-fits the Type IIb light curve.

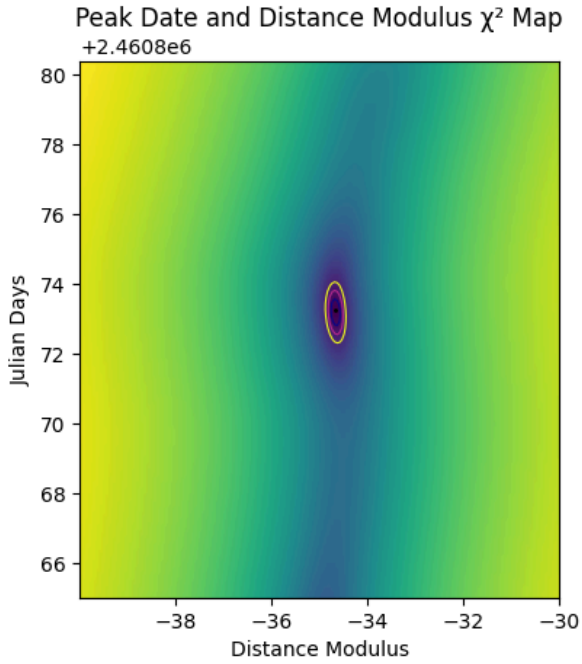

Figure 3: Chi-squared and distance modulus estimation of SN 2025mvn. The contours give an uncertainty of the day of peak and the distance modulus of the supernova. By finding the distance, it can aid in refining and calibrating various distance measurement techniques, including those that rely on other types of standard candles, giving scientists a chance in refining their understanding in the universe's scale and expansion history (J. S. W. Claeys et al. (2011)).

Table 1. Telescope and Filter Information

Dates	**Julian Date**	**Telescope**	**Filter**	**Exposure Time (sec)**
July 13	2460870.688	T24	Sloan g Sloan r	16x120 18x120
July 15	2460872.662	16-inch	Sloan g Sloan r	4x40 4x40
July 16	2460873.646	T24	Sloan g Sloan r	20x120 20x120
July 18	2460874.172	16-inch	Sloan g Sloan r	20x30 20x30
July 19	2460876.605	16-inch	Sloan g Sloan r	10x60 10x60

July 20	2460877.657	16-inch	Sloan g Sloan r	20x30 20x30
July 24	2460881.646	16-inch	Sloan g Sloan r	20x30 20x30
July 25	2460882.646	16-inch	Sloan g Sloan r	15x40 15x40
July 27	2460884.619	16-inch	Sloan g Sloan r	8x60 8x60
July 31	2460888.646	T24	Sloan g Sloan r	19x120 16x120

Table 1: Measurable observations collected over a 4-week period. This table provides information regarding the date, telescope model, filter, and exposure time (number of images x seconds).

Table 2. Calculated Green and Red Magnitudes of SN 2025mvn

Julian Date	**Green Magnitude**	**Green Error**	**Red Magnitude**	**Red Error**
2460870.688	18.0499	0.2112	16.4425	0.2471
2460872.662	17.4239	0.3323	16.8536	0.3683
2460873.646	17.5107	0.1708	16.6423	0.2146
2460874.172	17.6997	0.1229	16.3536	0.1461
2460876.605	18.6618	0.1693	16.8641	0.2060
2460877.657	18.7646	0.2379	18.3000	0.2900
2460881.646	17.8183	0.1650	16.3612	0.1951
2460882.646	18.0552	0.2755	17.1128	0.3123
2460884.619	17.7559	0.4984	17.2477	0.4738
2460888.646	17.9585	0.2012	16.6248	0.2309

Table 2: Calculated apparent brightness using the transformation equations. This table presents the calculated apparent magnitudes of SN 2025mvn across ten observation days. These values were obtained using the transformation equation.

Table 3: The Calculated Slopes and Intercepts Using Calibration Stars

Date	**Tgr**	**Cgr**	**Tg**
July 13	0.7204	0.2808	0.2136
Jul 15	0.0863	0.4714	-0.0849
Jul 16	0.7528	0.5763	0.2287
Jul 18	0.7988	0.2763	-0.0325
Jul19	0.7333	0.4545	0.1464
Jul 20	-0.0455	0.5362	0.3292
Jul 24	0.7537	0.2486	-0.1858
Jul 25	0.3252	0.3298	0.3443
Jul 27	-0.0173	0.3205	1.1384
Jul 31	0.7246	0.7226	0.1857

Table 3: Best-fit slopes (T) and the y-intercepts (c). The calculated slopes and intercept values derived from the calibration stars observed on the ten days. These were calculated using the transformation equation and are used to analyze atmospheric extinction, true color index, and filter set.

Table 4: Reduced Chi Squared of Light Curve

Supernova Light Curve	Optimized Chi-Squared
Type Ia	7.265
Type Ib	6.246
Type IIb	1.501
Type IIl	6.083
Type IIp	6.707

Table 4: Calculated Chi-Square values of observational points fitting to SNe light curve models. The table presents the total chi-squared error between the points and the light curve, with a higher value resulting in a better fit.

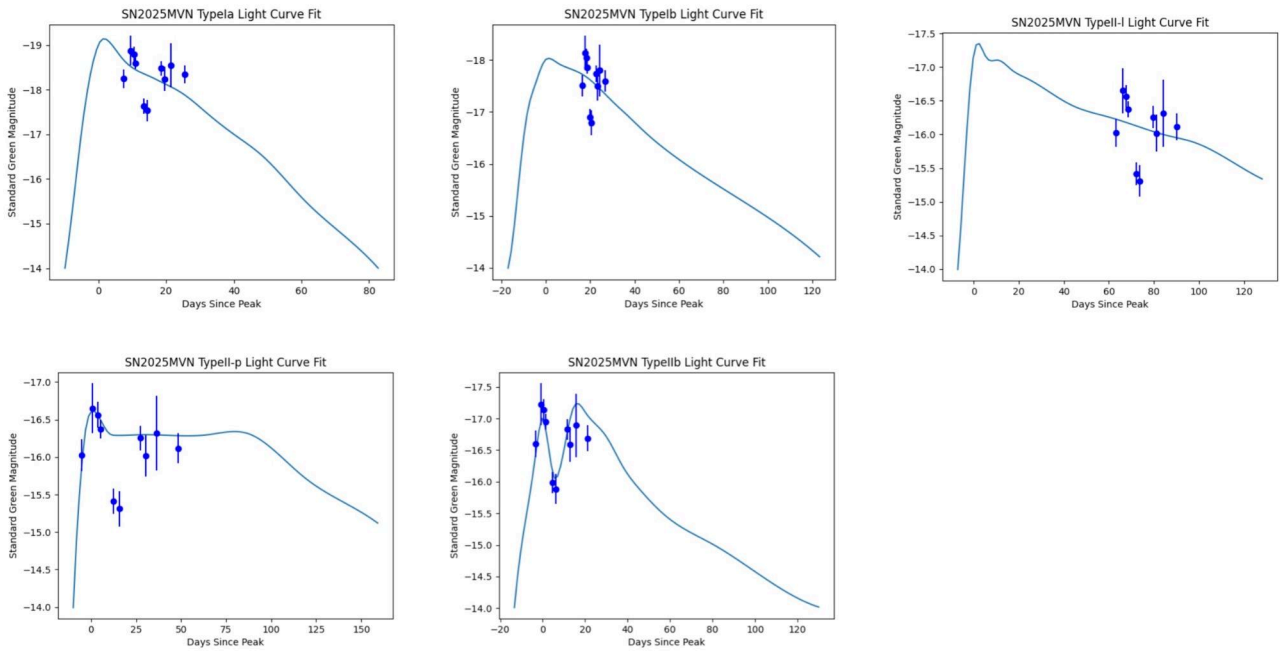

Figure 4: Observation data fitted to different light curves. The Sloan green (g) apparent magnitudes of the observations were fitted to five different supernovae models to determine the type of SN 2025mvn. The following types include Ia, Ib, II-l, IIp, and IIb. It is seen that Type IIb fits best by eye as well as least amount of error (chi-squared value of 1.501).

Conclusion

Through the performed photometric analysis, the observed brightness of supernova SN 2025mvn was plotted overtime and classified as a Type IIb supernova with a distance modulus of -34.673 ± 0.075, with a y-shift of approximately 2460873.267 ± 0.26 (**Figure 3**), and a distance of 1.165 ± 0.039 x 10^{-6} parsecs away from Earth.

When fitting the gathered magnitudes of SN 2025mvn to models of Type Ia, Ib, IIb, II-L, and II-P supernovae, a Type IIb supernova light model fit provided the lowest chi-squared value (chi-squared = 1.501), which is significantly less than the other light curve fits. This makes Type IIb the most likely candidate for the identity of SN 2025mvn. The majority of the calculated Tgr and Cgr were close to 1 and 0, indicating the data displayed minimal atmospheric effect. This strong correlation between the apparent and standard brightness increases the accuracy of the observational data. In addition, the average Tg from the observation data were close to 0, indicating a strong filter status, which further strengthens the accuracy of the observations (**Table 3**). Even after omitting the weakest points and refitting onto the light curve models, the results, nevertheless, displayed the best-fit with Type IIb supported by the lowest chi-squared value, further reinforcing the classification of SN 2025mvn is a Type IIb supernova.

Implications could include if spectroscopy were to be performed on the target, it would display strong hydrogen lines which would fade and give way to strong helium lines as the supernova evolved. It also demonstrates the star had lost most, but not all, of its hydrogen envelope prior to core collapse, suggesting either a binary companion or strong stellar winds from the progenitor star. By comparing the color magnitude charts formed from the data shows a consistently lower magnitude in the red charts than in the green charts, SN 2025mvn is brighter in the red visible part of the spectrum, revealing the progenitor star may have been a large, extended red supergiant with significant thin hydrogen envelopes (Claeys et al., 2011).

This project has contributed to the growing database of extragalactic supernovae by fitting the aforementioned light curve. SN 2025mvn is a particularly useful addition since it is likely a Type IIb supernova, a relatively rare type of supernova whose mechanisms are not yet entirely understood. Further research on this classification of supernovae can provide insights on the physics of binary interactions like stellar mass loss and the transferring of chemical elements within a star’s core.

As for further research, more could be learned about SN 2025mvn by continuing observations of its brightness over time to increase the certainty of the light curve fit. Spectroscopy could be conducted to deeper understand the chemical composition of this particular supernova in order to generate models for how supernovae evolve as a whole.

Acknowledgments

We would like to express our deepest gratitudes to Dr. Michael Faison, director of the Leitner Family Observatory and Planetarium for his contribution to every step of this research project. It is because of him that we were able to use the 0.4m Ritchey-Chretien Telescope and the T24 Sierra Remote Observatory telescope through iTelescope to conduct research on SN 2025mvn.

We would also like to thank Mr. Michael Warrener for his endless help and support, and especially for his organization and patience. He was always there to help us with programming errors or difficulties with iTelescope, and he ensured that the observing log was always up-to-date.

Finally, thank you to the teacher assistants and supporting staff: Kyra Bettwy, Ellis Eisenberg, and Nikki Wu, as well as Will Cerny and Surendra Bhattarai and their help with using the 0.4m Ritchey-Chretien Telescope. Their support and kindness were crucial for the completion of this research project.

References

Aavso.org. (2020). *Photometric Filter Selections | aavso*. [online] Available at: https://www.aavso.org/photometric-filter-selections [Accessed 18 Sep. 2025].

Claeys, J. S. W., de Mink, S. E., Pols, O. R., Eldridge, J. J., & Baes, M. 2011, Astronomy Astrophysics, 528, A131, doi: https://doi.org/10.1051/0004-6361/201015410

ESA. 2018, www.esahubble.org. https://esahubble.org/images/potw1843a/

Mattson, B., Ptak, A., & Myers, J. D. 2013, imagine.gsfc.nasa.gov. https://imagine.gsfc.nasa.gov/science/toolbox/timing1.html

Rochester. 2025, Rochesterastronomy.org. https: //rochesterastronomy.org/supernova.html#2025mvn

Support. (2021). *Telescope 24*. [online] Available at: https://support.itelescope.net/support/solutions/articles/231907-telescope-24 [Accessed 19 Sep. 2025].